HiSST: 3rd International Conference on
High-Speed Vehicle Science Technology
14 -19 April 2024, Busan, Korea

TSTO Launcher for small Satellites

Lakshmi Narayana Phaneendra Peri[1], Francesco Margani[2] Luca Armani[3], Sasi Kiran Palateerdham[4], and Antonella Ingenito[5]*

[1,4,5] School of Aerospace Engineering University of Rome "La Sapienza", Rome 00138, Italy
[2,3] GAUSS Srl, Rome 00138, Italy

Corresponding author: Antonella Ingenito
Email address: antonella.ingenito@uniroma1.it
Tel: +39 3346068243

Abstract

This study proposes a Two Stage to Orbit (TSTO) launcher aimed at deploying small payloads into low Earth orbit (LEO) by leveraging Rocket Based Combined Cycle (RBCC) technology. The proposed launcher comprises three stages: a solid rocket booster in the first stage, a reusable dual-mode ramjet-scramjet in the second stage, and a hybrid rocket in the third stage, enabling the insertion of payloads weighing approximately 100 kg into orbit. The design of the second stage is based on the VDK methodology, particularly focusing on the Kuckeman tau non-dimensional parameter. Additionally, mission analysis has been conducted to validate the launcher's capability to meet mission requirements effectively.

Keywords: *Space launchers, dual mode ramjet, rockets, Two stage to orbit, micro-satellite, RBCC*

1. Introduction

As technology advances, satellites are becoming smaller and more cost-effective, leading to an increase in the number of small satellite launches. [1-3]. Launchers capable of delivering a small payload into a customized orbit on short notice are experiencing growing demand [4-6]. This demand can be met through the application of Rocket Based Combined Cycles (RBCC). RBCC engines integrate conventional rockets with high thrust-to-weight ratio and air-breathing engines with high specific impulse [7]. Incorporating a scramjet or a dual mode ramjet (DMR) during trans-atmospheric flight reduces the overall mass of the launcher by eliminating the need to carry oxidizer onboard, as it utilizes oxygen available in the atmosphere. This, in turn, enhances the payload capacity [8-11]. However, supersonic combustion remains a critical challenge, particularly in achieving efficient mixing and combustion of fuel and air within short lengths, which is essential for minimizing total pressure losses [12-14]. The limited residence time inside the scramjet combustor, typically on the order of milliseconds, worsens these challenges [15, 16]. Introducing cavity concepts after the injectors increases jet penetration depths, enhances recirculation zones, increases fuel-air residence time, improves flame anchoring and enhances combustion efficiency, addressing issues such as high injection angles (90º) leading to total pressure loss, and lower injection angles (30º and 60º) causing reduced net thrust [17, 18, 19, 20]. As for as hybrid Rocket Engines (HREs), among various propulsion systems, these offer advantages of both Liquid Rocket Engines (LREs) and Solid Rocket Motors (SRMs): safety, reliability, simplicity, eco-friendliness, higher specific thrust, and specific impulse. Throttling capabilities allow precise

manoeuvring, enabling satellite insertion into desired orbits at any inclination [21-27]. Extensive research has focused on using paraffin as an HRE fuel due to its decent specific impulse and reduced environmental impact, particularly in terms of absence of harmful emissions such as Hydrogen chloride (HCl), Sulphur oxides (Sox), and Nitrous Oxide (N2O). Nitrous Oxide is considered as the oxidizer due to its self-pressurizing properties, eliminating the need for additional pressurizing systems and reducing overall vehicle mass [28, 29].

2. TSTO Launcher mission profile

The primary objective of the launcher is to transport a 100 kg payload to a designated low Earth orbit at an altitude of 200 km. To achieve this goal, the launcher has been divided into three stages. The first stage employs a solid rocket booster, which operates until the vehicle reaches an altitude of 17 km. At this altitude, the second stage starts, featuring a reusable dual-mode ramjet-scramjet configuration. This stage operates until reaching the upper atmosphere, approximately 70 km in altitude, where oxygen levels become scarce. Following this, the third stage, a hybrid rocket housed within the scramjet's launch bay, delivers the satellite to the designated 200 km altitude orbit. Upon completion of its mission, the scramjet of the second stage returns to Earth's surface and can be utilized for future launch missions. Fig. 1 outlines the overall mission profile of the launcher.

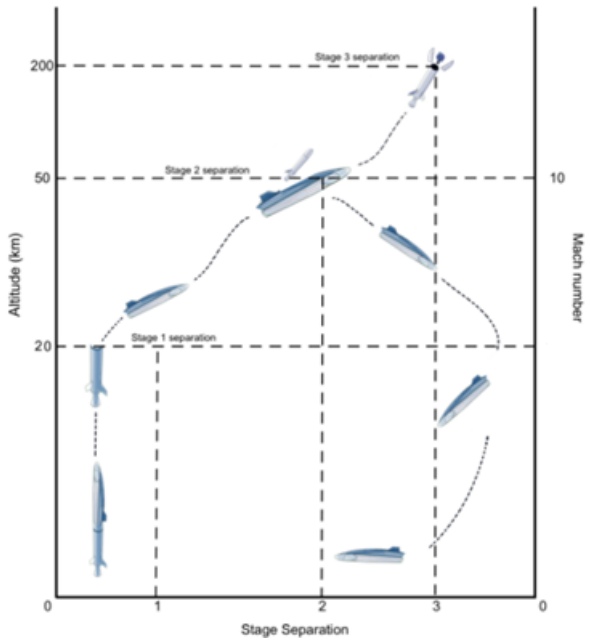

Fig 1. Mission profile of the launcher

The objective of this section is to assess and validate a potential launch trajectory by analysing key parameters of the rockets, including mass, thrust, and specific impulse, with a particular focus on the second stage equipped with a Ramjet-Scramjet dual-mode engine. The primary constraints revolve around the capabilities of this second stage engine, with a selected starting Mach number of 4 and a final Mach number of 9. Additionally, altitude plays a critical role, as the dual-mode engine's effectiveness is optimal within the altitude range of 20km to 70km.

To accurately compute the rocket's flight trajectory, a two-dimensional calculation code was developed, leveraging equations governing the dynamics of the launcher represented as a material point. A time-stepping approach was employed to calculate variations in velocity, position, and mass incrementally. Furthermore, a decomposition into directional components was adopted to enhance computational

efficiency and accuracy, x and y where y represents the altitude while x the distance from the launch site.
To ensure the highest level of accuracy in the calculations, drag was incorporated and computed using the following formula:

$$D_x = \frac{1}{2}\rho {V_x}^2 C_d S$$
$$D_y = \frac{1}{2}\rho {V_y}^2 C_d S$$

The change in drag coefficient C_d in function of the Mach number, ρ density, T temperature and the speed of sound, function of the altitude, is calculated based on the International Standard Atmosphere to ensure consistency and good accuracy.

The rocket's thrust, T, is initialized by implementing the initial launch angle θ: $T_x = Tcos(\theta)$, $T_y = Tsin(\theta)$. The implemented dynamics equations are:

$$dV_x = \left(\frac{T_x}{m_0} - \frac{D_x}{m_0} - g\right) dt$$
$$dV_y = \left(\frac{T_y}{m_0} - \frac{D_y}{m_0} - g\right) dt$$
$$dx = dV_x * dt$$
$$dy = dV_y * dt$$
$$dm = \dot{m} * dt$$

The mass flow rate $\dot{m}$ has been calculated for the rocket by:

$$\dot{m} = \frac{T}{I_{sp} * g}$$

for the airbreathing vehicle by:

$$\dot{m} = \frac{T}{(I_{sp} * g) - V}$$

The variables of position, velocity and mass are updated iteratively using:

$$V_{xi} = V_{x(i-1)} + dV_x$$
$$V_{yi} = V_{y(i-1)} + dV_y$$
$$x_i = x_{i-1} + dx$$
$$y_i = y_{i-1} + dy$$
$$m_{0i} = m_{0i-1} - dm$$

The angle of flight was calculated at each step as a function of the velocity components V_x, V_y:

$$V = \sqrt{{V_x}^2 + {V_y}^2}$$
$$\theta = \cos^{-1}\left(\frac{V}{V_x}\right)$$

To optimize the trajectory of the launch, two different types of rocket guidance were employed. The first method is the gravity turn, where the thrust components of the rocket, T_x, T_y, are aligned with the angle θ. Alternatively, the thrust components can be assigned a constant angle θ, resulting in a trajectory with a constant thrust direction.
The modelled launcher consists of three stages, necessitating consideration of three distinct flight phases with varying input parameters. Notably, during the separation of each stage, there is a sudden decrease in mass, which must be accounted for. Specifically, the burn-out times of the three stages were taken into consideration: $t_{bo1}, t_{bo2}, t_{bo3}$
From these, considering the interstage time t_{is}, the end point of each flight phase was calculated:

$$t_{f1} = t_{bo1} + t_{is}$$

$$t_{f2} = t_{f1} + t_{bo2} + t_{is}$$
$$t_{f3} = t_{f2} + t_{bo2} + t_{is}$$

Within these stages, the equations of dynamics expressed above were then calculated. Considering then the empty masses of the different stages m_{01}, m_{02}, m_{03}, and the total mass m_0, it was possible to calculate the detachment of stages as:

$$m_0 = m_0 - m_{01} \ at \ t = t_{f1}$$
$$m_0 = m_0 - m_{02} \ at \ t = t_{f2}$$
$$m_0 = m_0 - m_{03} \ at \ t = t_{f3}$$

Table 1 shows the configuration of the rocket achieved through some iteration to fulfill the mission requirements. m0 is the mass of the first stage without the payload mass.

Table 1. Three stage rocket configuration

	m_0 (kg)	m_{prop} (kg)	T (N)	Isp (s)	t_{bo} (s)	ΔV (m/s)
Stage 1	5910	3340	342476	261	25	2135
Stage 2	1952	314	70000	1250	55	3285
Stage 3	616	416	13800	331	98	3655

The total mass of the launcher is 5910 kg, including a 100 kg payload. The total mission duration is approximately 182 seconds, with an interstage time of 2 seconds. The total change in velocity (ΔV) required for the mission is calculated by summing the values for each stage, determined using the Tsiolkovsky equation. This cumulative value ensures the spacecraft can successfully enter orbit. The computed ΔV value is compared with the theoretical calculation, revealing the differences attributable to drag and gravity losses, as shown in Table 2.

To compute the correct trajectory, a gravity turn guidance is employed for the first stage. For the second and third stages, constant thrust angles of 12° and 20° respectively are defined. The solid booster is designed to reach a height of approximately 17,000 m with a specific Mach number of 4, enabling proper ignition of the ramjet. If the Mach number exceeds the ramjet's operational limit, it transitions to a scramjet configuration, engaging between Mach 7 and Mach 9, reaching a final altitude of 63,000 m. The hybrid third stage is designed to achieve an altitude of around 200,000 m in horizontal flight with a circular orbital velocity.
The rocket's trajectory is shown in Figure 2, Mach and velocity are shown in Figure 3.

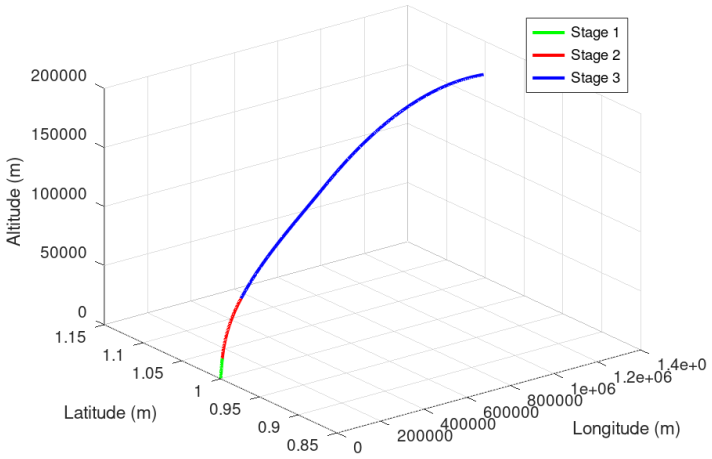

Fig 2. Trajectory

The trajectory of the launcher is shown in Fig. 2 the green line represents the first stage, the red line the dual-mode engine stage, and the blue line represents the final stage and payload. These stages are dimensioned to achieve an altitude of 200 km with horizontal flight.

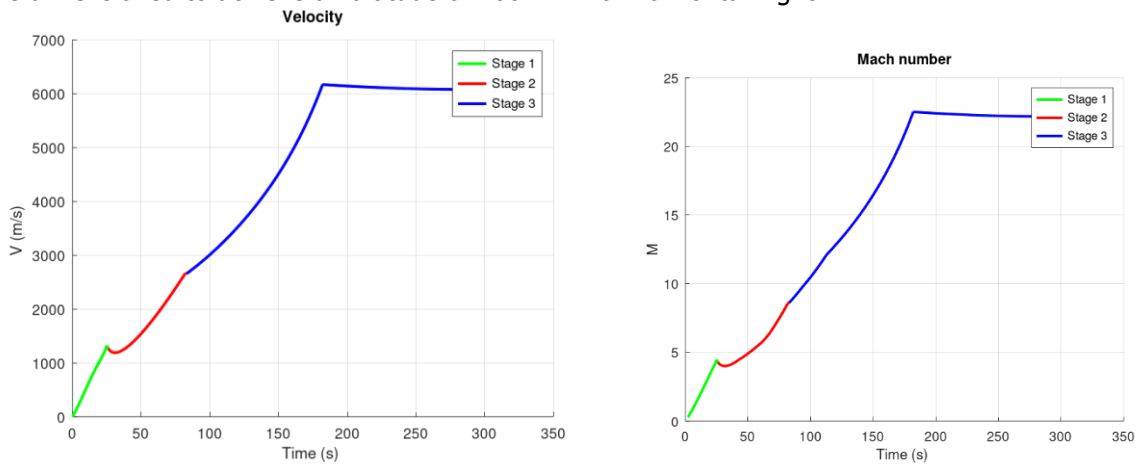

Fig 3. Velocity and Mach number in function of the time

Table 2. Velocity and Mach number in function of altitude.

Stage	Altitude (m)	V (m/s)	M
1	10000	998	3.3
2	20000	1195	4.1
2	40000	1632	5.13
2	60000	2514	8.2
3	80000	3150	11.2
3	100000	3936	14.3
3	150000	6150	22.4
3	200000	6076	22.2

Focusing on the second stage it is possible to compute the starting Mach number, $M_{start} = 4.2$ and final Mach, $M_{end} = 8.7$. The best choice is to use a ramjet-scramjet dual mode engine, that combine the efficiency of the ramjet until $M = 6$ and the supersonic combustion of the scramjet from $M = 6$ to $M = 8.7$. Fig. 4 shows the mass of the launcher changes during the mission. After the burn out of the third stage, the only remaining part is the payload with a mass of 100 kg.

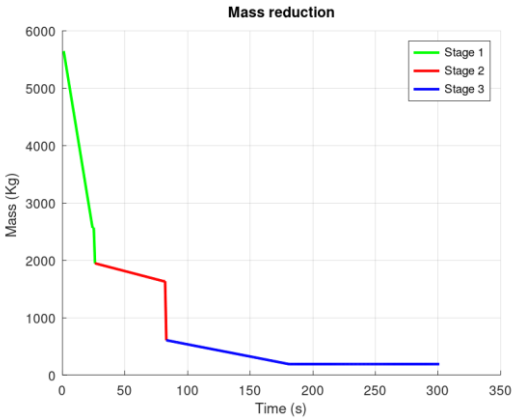

Fig 4. Mass reduction

3. Launcher sizing

Starting from the mission analysis, a MATLAB code has been developed to design each stage.

3. 1. Design of the Fist stage

The propellant composition for the solid rocket booster is defined as follows:

- HTPB (Hydroxyl-terminated polybutadiene): 12%
- AP (Ammonium Perchlorate): 68%
- Al (Aluminum): 20%

CF and Isp (implemented in the mission analysis calculations) have been calculated by the CEA code, assuming an expansion ratio of e = 16. Input parameters are given in the Table 3 below.

Table 3. Input parameters for the first stage

Fuel composition	HTPB/AP/Al
Density kg/m3	1854.5536
a [mm/s]	2.772
n (pressure in MPa)	0.560
Ae_At	16.000000
Pc [atm]	100
Isp [s]	260
CF	1.629500
rdot[m/s]	0.010065

Table 4. Preliminary size of solid booster

GRAIN	Dgint[m]	0.410790
	Dgext[m]	0.900000
NOZZLE	Dthroat [m]	0.164758
	Dexit [m]	0.659032
	Lcon [m]	0.247137
	Ldiv [m]	0.922328
	Lbooster [m]	3.525663

3. 2. Design of the Second stage

In order to design the second stage, the VDK (Vanderkerkhove)/HC approach has been applied. This approach is generally used for sizing of high-performance hypersonic, subsonic aircraft and reusable space launchers. In this approach, sizing begins with mission distance, payload, and DV, to obtain a figure of merit (τ) of the entire vehicle. For a given mission requirement, more than one configuration has been found, and it is the constraints of the type of mission (commercial aircraft, space aircraft, launcher...) that will define the "best configuration". Solutions of GW, W_{fuel} and W_{str} as a function of S_{plan} are shown in Fig. 4.

In order to identify the solution that was able to satisfy the mission analysis, a Kuckemann τ of 0.08 has been chose. For this tau, the propellant weight is 314 kg, and the overall weight is 2563,94 kg, i.e. with an error of 0.15% with respect to that obtained by the mission analysis requirements.

The burning time is about 55 s. The total length is about 8 m, including also the first stage. Weights for the second stage are given in the Table 5.

Table 5. Preliminary size for the second stage

Wpay[kg]	616.000000
GWramjet [kg]	2563.94
Wsys [kg]	93.444174
Weng [kg]	40.509858
Wfuel[kg]	314.906229
Wstr [kg]	1500.696640

Thrust, total vehicle length, fuel weight, specific impulse as a function of τ are shown in Fig. 6.

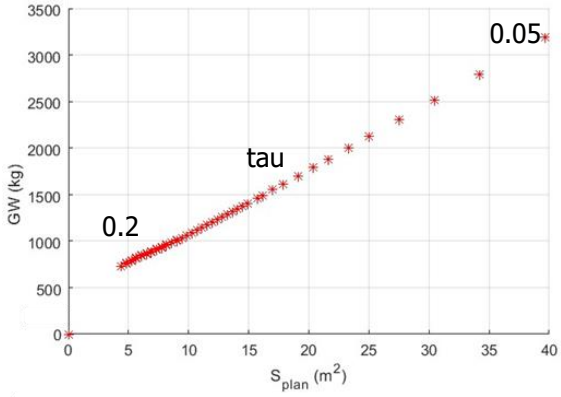

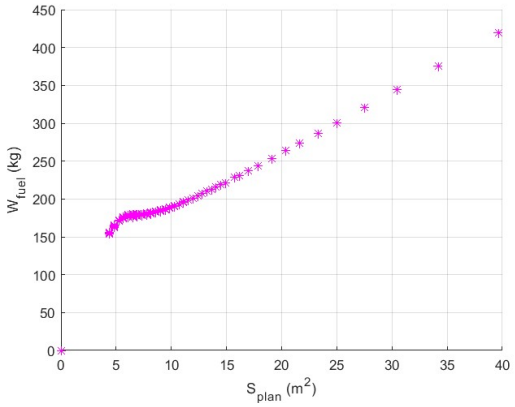

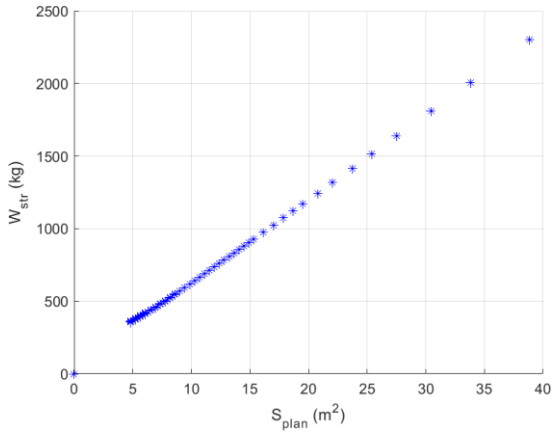

Fig 5. GW, W_{fuel}, W_{str} (kg) vs Splan for the second stage

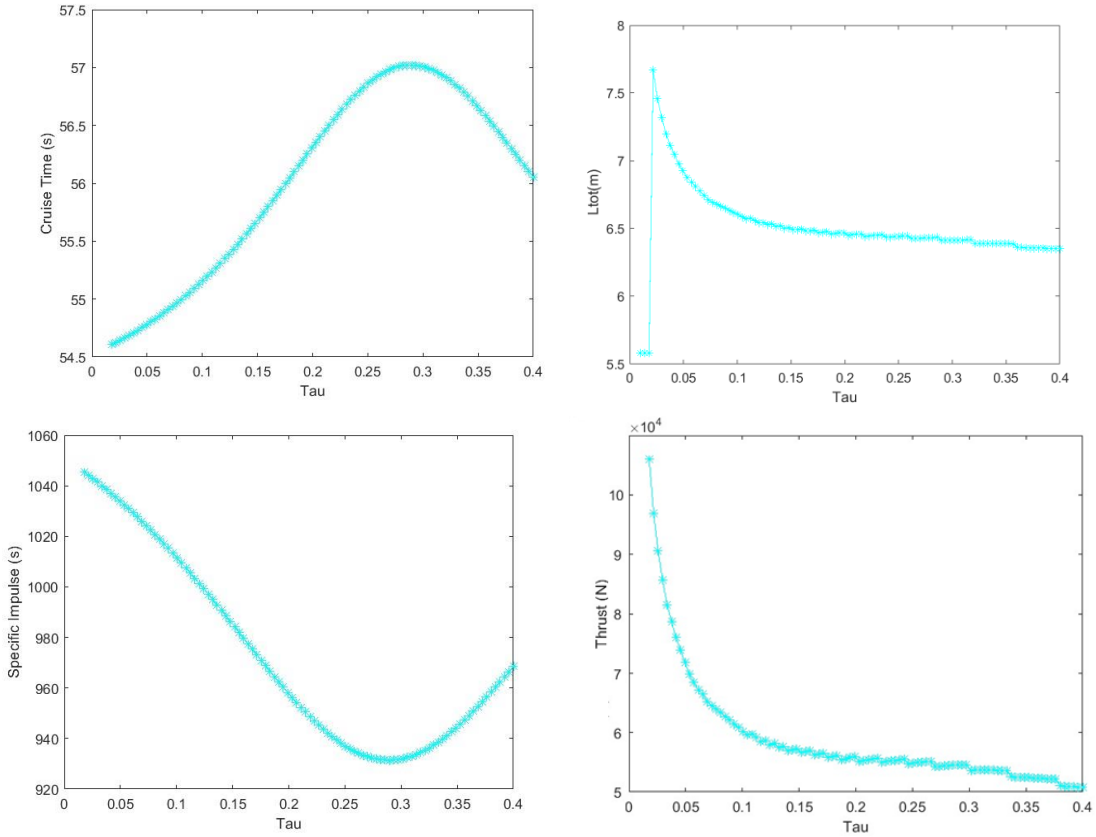

Fig 6. burning time, Ltot, Isp, Thrust vs τ for the second stage

To ensure the accuracy of the preliminary design, it is imperative to determine whether the inlet can deliver the required air mass flow rate at the appropriate pressure and temperature conditions, while adhering to dimensions suitable for the sized launcher. For the scramjet, based on a 2D analysis, a two-ramp inlet, with the first ramp angle of 6º and the second ramp angle incrementing by 8º, has been designed using MATLAB code, where the operational conditions of the scramjet are considered at 6.8 Mach (see Fig. 7).

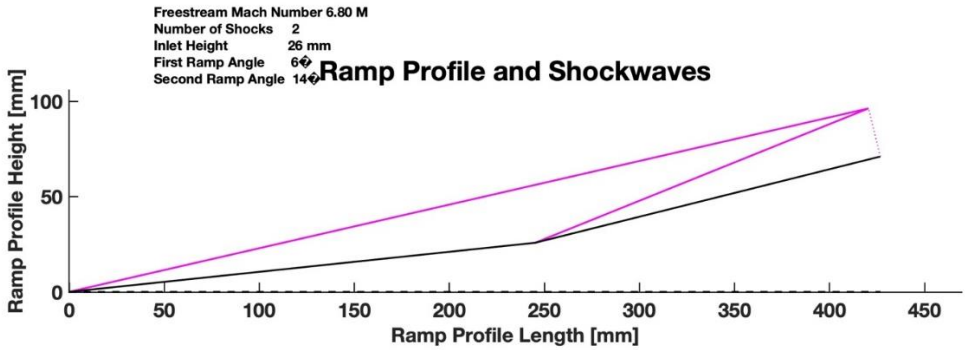

Fig 7. Scramjet intake ramps profile

Downstream of the intake, an axi-symmetric cavity based circular combustor is considered for the launcher (Fig. 8): this should allow an efficient combustor with low total pressure losses.

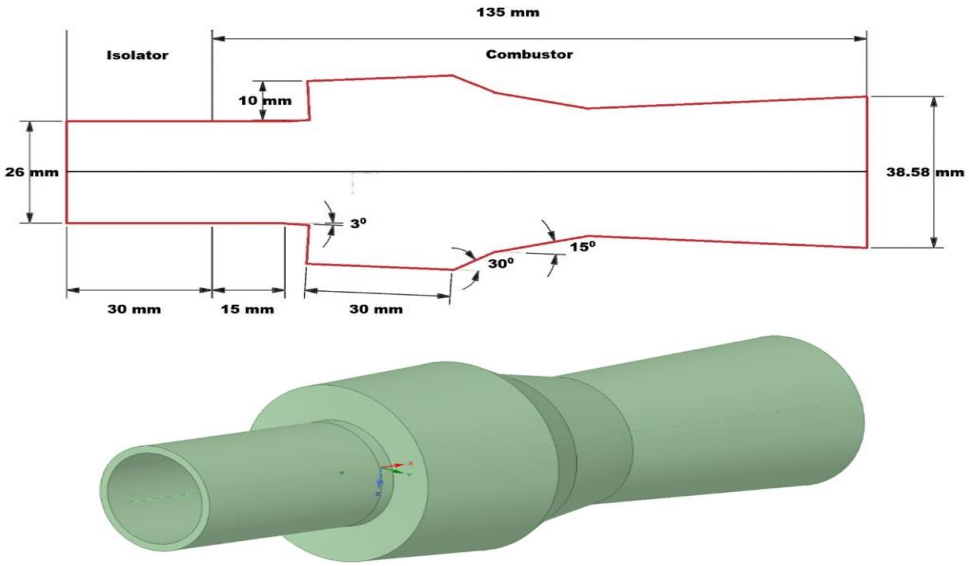

Fig 8. Configuration of the axi-symmetric cavity based circular combustor

3. 3. Design of the Third stage

For the third stage, assuming paraffin as fuel and nitrous oxide (N2O) as oxidiser, the hybrid rocket engine (HRE) was designed. Table 6 shows the input data to design the HRE.

Table 6. Input data for third stage

Parameter	Value
Thrust	13800 N
Chamber pressure	8000000 Pa
Burning time	98 s
Mixture ratio	4
Number of combustion ports	1
Specific Impulse	331.75 s
Thrust coefficient	1.99
Nozzle expansion ratio	174.63

Flame temperature	3313 k
Heat capacity ratio	1.575
Initial Gox	225 kg / m^2.sec
Combustion gases molecular weight	26.983 kg/mol
Fuel	Paraffin
Oxidizer	Nitrous oxide
Fuel density	900 kg/m3
Regression rate coefficient (a)	0.1781.10-3
Regression rate exponent (n)	0.543
Oxidizer density	Function of the temperature

Utilising the data provided from National Institute of Standards and Technology (NIST) [32], the density of nitrous oxide is calculated in function of temperature as it saturates at the ambient conditions. A 5% of pressure losses in feeding line is assumed. Sizing has been done accounting for the pressure history and the O/F ratio changes within the rocket during the burning time.

Table 7. Nozzle design

Design		
Fuel	Fuel port diameter	0.145198 m
	Fuel final diameter	0.461951 m
	Fuel length	0.446427 m
	Fuel mass	62.036096 kg
Tank	Oxidizer mass	372.216577 kg
	Tank volume	0.269908 m^3
	Tank diameter	0.800000 m
	Tank length	0.5143 m
Nozzle	Throat diameter	0.034931 m
	Exit diameter	0.110462 m
	Convergent length	0.055134 m
	Divergent length	0.796830 m
Injector	Injection area	3.822309e-05 m^2
	Orifice diameter	0.002206 m
	Number of holes	10
	Discharge coefficient	0.660000
Hybrid	Case mass	9.159371e+01 kg
	Pressurizing Mass	28.853843 kg
	Pressurizing tank mass	4.733861e+00 kg
	Helium mass	3.894202e-01 kg
	Helium tank mass	6.267414e+00 kg
Stage	Stage length	2.610223e+00 m
	Total Mass	642.815842 m
	External Diameter	8.537215e-01 m

Table 7 shows the results for the hybrid rocket. A 12% of ullage volume is assumed to design the oxidizer tank. A discharge coefficient of 0.66 is assumed. The convergent section has an inclination of 45° and 15° for divergent part. The geometry of the hybrid rocket engine is represented in the Fig. 9.

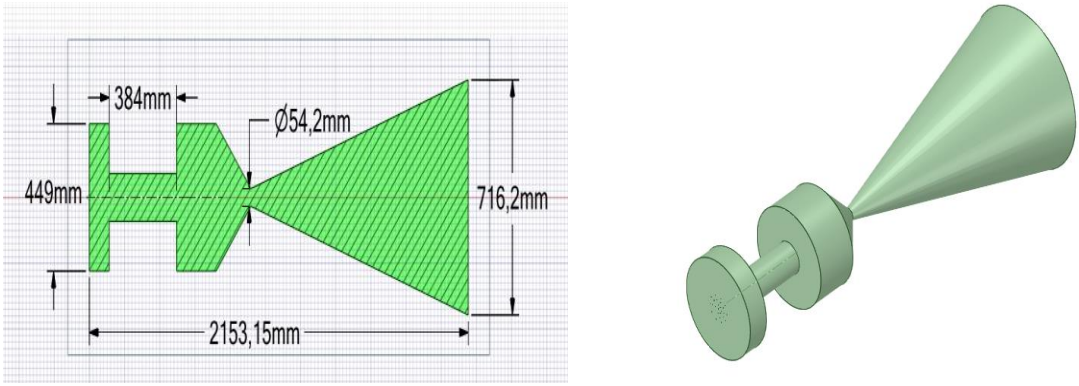

Fig 9. Schematic view of Hybrid Rocket Motor

Fig. 10 and Fig. 11 show the regression rate, fuel mass flow rate, Characteristic velocity, Chamber pressure, Thrust, Specific Impulse, oxidiser to fuel ratio vs time.

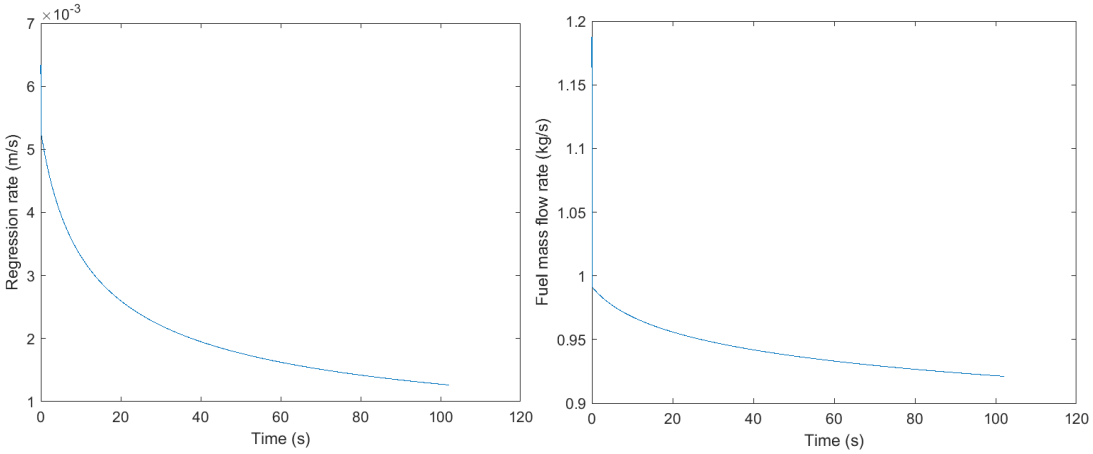

Fig 10. Regression rate, fuel mass flow rate vs time

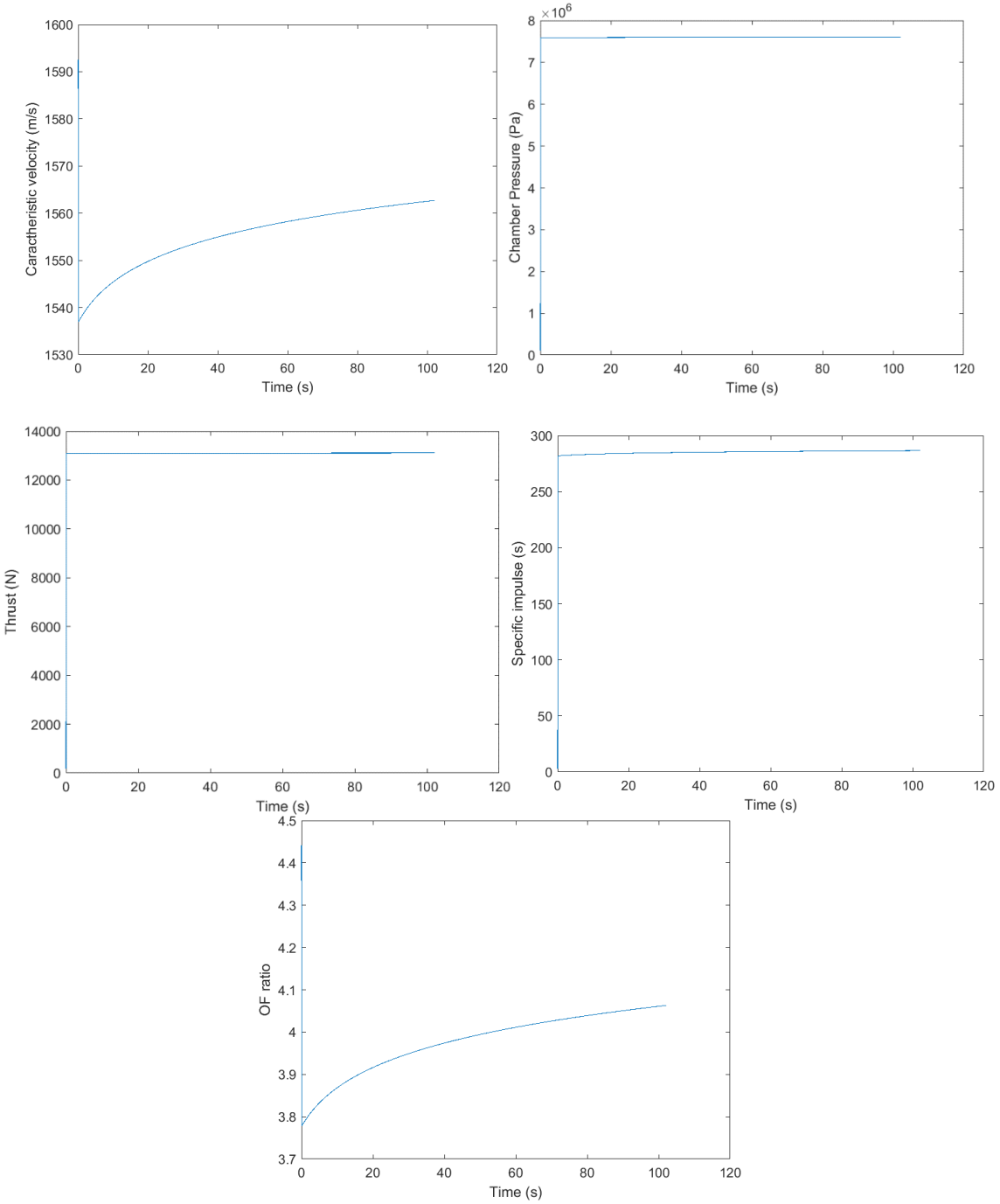

Fig 11. Characteristic velocity, Chamber pressure, Thrust, Specific Impulse, oxidiser to fuel ratio vs time

4. Final configuration of the TSTO launcher

Summarizing the previous work, the launcher employs a solid booster at the top, succeeded by a ramjet operating from Mach 4 until it reaches scramjet operating conditions between Mach 6 to 9. Following the scramjet phase, the hybrid rocket is ignited to achieve a 200 km altitude at the required Delta-V. The dual-mode ramjet necessitates an adaptive intake system. During ramjet operation, both intake

ramps are positioned at 1 and 2, allowing compressed air to enter the combustor and decelerate to subsonic speeds. In scramjet mode, intake ramps 1 and 2 are positioned at 1' and 2', while the cowl lip position changes from 3 to 3', enabling air to enter the combustion chamber and decelerate while maintaining supersonic velocities. Furthermore, adjustments are made to the nozzle during the exit of combusted gases from the scramjet engine, shifting the upper part from N1 to N1' and the lower part from N2 to N2'.

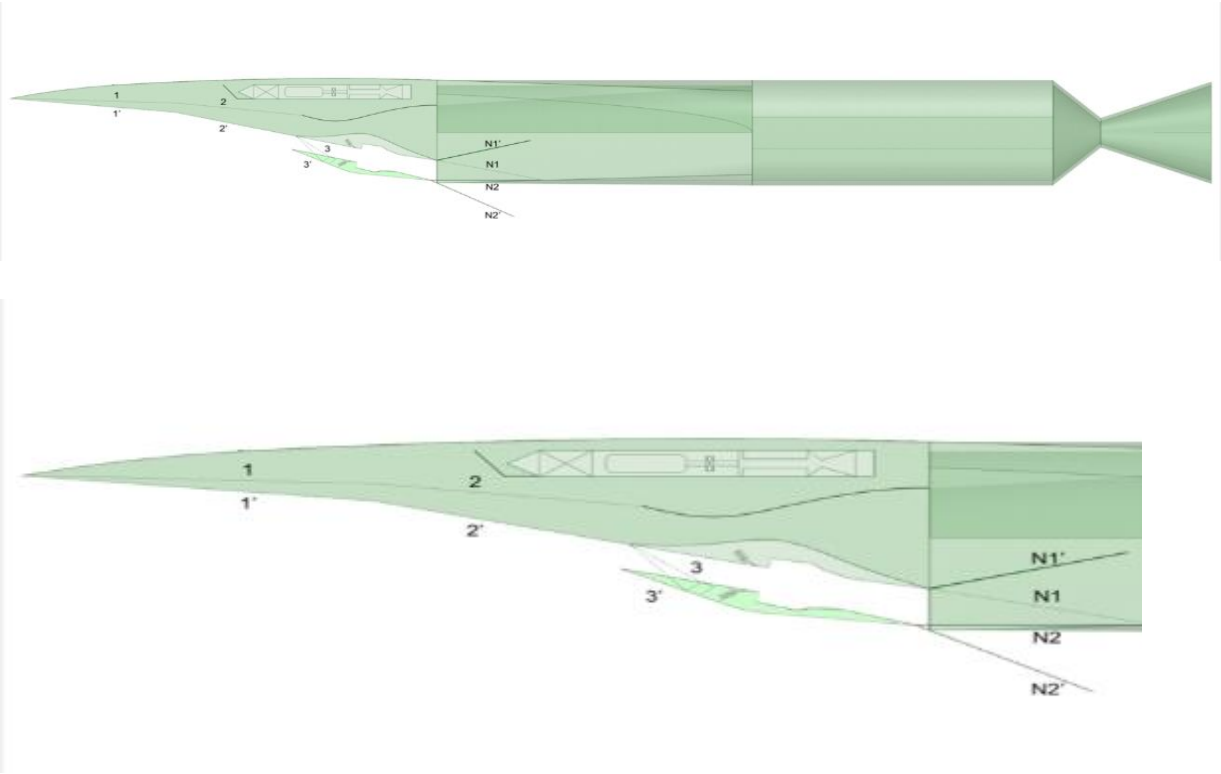

Fig 11. Layout of the proposed launch vehicle

5. Conclusion

The study investigate the feasibility of a Two Stage to Orbit (TSTO) launcher capable of transporting a 100 kg payload into its designated orbit. The launcher's total mass, including payload, has been found to be 5910 kg, with a mission duration of approximately 182 seconds and an interstage time of 2 seconds.
Starting from the trajectory analysis the solid booster operates from take-off to Mach 4 reaching an height of approximately 17,000 m. After the first stage is burned out, a dual mode ramjet starts to operate until Mach 7, then a scramjet starts until Mach 9, reaching a final altitude of 63,000 m. The hybrid rocket engine is then ignited to achieve an altitude of around 200,000 m in horizontal flight reaching a final circular orbital velocity.

To optimize each stage's performance, a gravity turn guidance is employed for the first stage, and constant thrust angles of 12° and 20° are defined for the second and third stages, respectively.

Utilizing MATLAB and computational tools, each stage of the launcher is meticulously designed, considering factors such as propellant composition, nozzle design, and engine specifications.
In conclusion, the integrated approach to launcher design, combining solid booster, scramjet, and hybrid rocket technologies, promises improved performance and mass budgeting for space missions.

References

1. OfficeofCommercialSpaceTransportation(AST)andtheCommercialSpaceTransportationAdvisory Committee(COMSTAC), *2015 Commercial Space Transportation Forecasts*, May, Office of Commercial Space Transportation, Washington, DC, 2015.
2. McIntyre, S., "Andy and Feast , Simon (2016) How to launch small payloads ? Evaluation of current and future small payload launch systems . In : 14th and future small payload launch systems," 2016.
3. Crisp,N.H.,Smith,K.,andHollingsworth,P.,"Launchanddeploymentofdistributedsmallsatellitesystems,"*ActaAstronautica*, Vol. 114, 2015, pp. 65–78. doi:10.1016/j.actaastro.2015.04.015, URL http://dx.doi.org/10.1016/j.actaastro.2015. 04.015.
4. Maddock, C., Toso, F., Ricciardi, L., Mogavero, A., Lo, K. H., Rengarajan, S., Kontis, K., Milne, A., Evans, D., West, M., and McIntyre, S., "Vehicle and Mission Design of a Future Small Payload Launcher," *21st AIAA International Space Planes and Hypersonics Technologies Conference*, , No. March, 2017, pp. 1–20. doi:10.2514/6.2017-2224, URLhttps: //arc.aiaa.org/doi/10.2514/6.2017-2224.
5. Kuhn, M., Müller, I., Petkov, I., Oving, B., van Kleef, A. J., Verberne, C. J., Haemmerli, B., and Boiron, A., "Innovative European Launcher Concept SMILE," *21st AIAA International Space Planes and Hypersonics Technologies Conference*, , No. March, 2017, pp. 1–14. doi:10.2514/6.2017-2441,URL https://arc.aiaa.org/doi/10.2514/6.2017-2441.
6. Charania, A. C., Isakowitz, S., Matsumori, B., Pomerantz, W., Vaughn, M., Kubiak, H., and Caponio, D., "SSC16-II-02 LauncherOne : Virgin Galactic ' s Dedicated Launch Vehicle for Small Satellites," *30th Annual AIAA/USU Conference on Small Satellites*, Logan, UT, 2016, pp. 1–8.
7. Zeyu Dong, Mingbo Sun, Zhenguo Wang, Jian Chen, Zun Cai. Survey on key techniques of rocket-based combiner cycle engine in ejector mode. Acta Astronautica 164 (2019) 51-68.
8. McIntyre, Stuart, et al. "How to launch small payloads? Evaluation of current and future small payload launch systems." 14th Reinventing Space Conference. 2016.
9. F. S. Billig, "Hypersonic propulsion concpets and challenges," in Hypersonic Systems and Testing, 2000.
10. W. H. Heiser and D. T. Pratt, Hypersonic Airbreathing Propulsion. *AIAA Education Series, American Institute of Aeronautics and Astronautics, Inc*, 1994.
11. R. Daines and C. Segal, "Combined rocket and airbreathing propulsion systems for space-launch applications," *Journal of Propulsion and Power*, vol. **14**, no. 5, 1998.
12. E. T. Curran, W. H. Heiser, and D. T. Pratt, "Fluid phenomena in scramjet combustion systems," Annu. Rev. Fluid Mech. **28**, 323 (1996).
13. F. S. Billig, "Research on supersonic combustion," J. Propul. Power **9**, 499 (1993).
14. J. Urzay, "Supersonic combustion in air-breathing propulsion systems for hyper- sonic flight," Annu. Rev. Fluid Mech. **50**, 593 (2018).
15. Seleznev, R.K.; Surzhikov, S.T.; Shang, J.S. A review of the scramjet experimental data base. *Prog. Aerosp. Sci.* 2019, **106**, 43–70.
16. Ren, Z.; Wang, B.; Xiang, G.; Zhao, D.; Zheng, L. Supersonic spray combustion subject to scramjets: Progress and challenges. *Prog. Aerosp. Sci.* 2019, **105**, 40–59.

17. Ben Yaker, A.; Hanson, R.K. Experimental Investigation of Flame-Holding Capability of Hydrogen Transverse Jet in Supersonic Cross Flow. *Symp. Int. Comb*. 1998, **27**, 2173–2180.
18. Owens, M.G.; Tehranian, S.; Segal, C.; Vinogradov, V.A. Flame-Holding Configurations for Kerosene Combustion in a Mach 1.8 Airflow. *J. Propuls. Power* 1998, **14**, 456–461.
19. Zhang, J.; Chang, J.; Tian, H.; Li, J.; Bao, W. Flame Interaction Characteristics in Scramjet Combustor Equipped with Strut/Wall Combined Fuel Injectors. *Combust. Sci. Technol*. 2020, **192**, 1863–1886.
20. Kim, C.H.; Jeung, I.S. Forced combustion characteristics related to different injection locations in unheated supersonic flow. *Energies* 2019, **12**, 1746
21. Cohen-Zur, A. and B. Natan, Experimental Investigation of a Supersonic Combustion Solid Fuel Ramjet. *Journal of Propulsion and Power*, 1998. **14(6)**: p. 880-889.
22. Savino, R. and G. Pezzella, Numerical Analysis of Supersonic Combustion Ramjet with Upstream Fuel Injection. *International Journal for Numerical Methods in Fluids*, 2003. **43**: p. 165-181.
23. Engelund, W.C., et al. Propulsion System Airframe Integration Issues and Aerodynamic Database Development for the Hyper-X Flight Research V ehicle. in *XIV ISOABE Conference*. 1999. Florence.
24. Lewis, M.J., Significance of Fuel Selection for Hypersonic Vehicle Range. *Journal of Propulsion and Power*, 2001. **17(6)**: p. 1214-1221
25. N.A. Davydenko, R.G. Gollender, A.M. Gubertov, V.V. Mironov, N.N. Volkov. Hybrid Rocket Engine: The benefits and prospects. *Aerospace Science and Technology* **11** (2007) 55-60.
26. A hybrid propulsion solution for a microsatellite to perform a capture maneuver in a Mars orbit / Levi Domingos, C. H. F.; Ingenito, A.. - (2020), pp. 1-17. (Intervento presentato al convegno AIAA Propulsion and Energy 2020 Forum tenutosi a USA) [10.2514/6.2020-3734].
27. Sutton, G.P.; Biblarz, O. Hybrid Propellant Rockets. In *Rocket Propulsion Elements*, 7th ed.; John Wiley & Sons: New York, NY, USA, 2001; pp. 585–593
28. Mario Kobald, Christian Schmierer, Helmut Ciezki, Stefan Schlechtriem, Elena Toson, and Luigi De Luca. "Viscosity and Regression Rate of Liquefying Hybrid Rocket Fuels". In: *Journal of Propulsion and Power* **33.5** (2017), pp. 1245–1251
29. Heejang Moon, Seongjoo Han, Youngjun You, Minchan Kwon. Hybrid Rocket Underwater Propulsion: A Preliminary Assessment. *Aerospace* 2019, **6**, 28, doi:10.3390/aerospace6030028.
30. Assis, S.M.; Suppandipillai, J.; Kandasamy, J. Transverse Injection Experiments within an Axisymmetric Scramjet Combustor. Int. *J. Turbo Jet-Engines* 2019.
31. Relangi, N.; Garimella, D.; Jayaraman, K.; Venkatesan, J.; Jeyakumar, S.; Ingenito, A. Numerical simulations of axisymmetric aft wall angle cavity in supersonic combustion ramjets. In *Proceedings of the AIAA Propuls, Energy* 2020 Forum, Virtual Event, 24–28 August 2020; pp. 1–15.
32. Choubey, G.; Patel, Om; Solanki, Malhar; Ingenito, Antonella; Devarajan, Yuvarajan; Tripathi, Sumit, Influence of cavity floor injection strategy on mixing improvement study of a splitter plate-assisted supersonic combustor, - In ENGINEERING ANALYSIS WITH BOUNDARY ELEMENTS. - ISSN 0955-7997. 2023, pp. 995-1012.
33. Relangi, N.; Ingenito, A.; Jeyakumar, S., The investigation of inclined aft wall cavities in a circular scramjet combustor - In: INTERNATIONAL JOURNAL OF ENGINE RESEARCH. - ISSN 1468-0874. - 24:4(2022), pp. 1300-1311. [10.1177/14680874221085059]
34. Relangi, N.; Ingenito, A.; Jeyakumar, S., The implication of injection locations in an axisymmetric cavity-based scramjet combustor - In: ENERGIES. - ISSN 1996-1073. - 14:9(2021), pp. 1-13. [10.3390/en14092626]
35. M. A. Karabeyoglu, D. Altman, and B. J. Cantwell. Combustion of liquefying hybrid propellants: Part 1, general theory. Journal of Propulsion and Power, 18(3):610–620, 2002